Ore Geology Reviews 73 (2016) 198–210

Contents lists available at ScienceDirect

Ore Geology Reviews

journal homepage: www.elsevier.com/locate/oregeorev

Metallogeny of the syenite-related Dongping gold deposit in the northern part of the North China Craton: A review and synthesis

Zhiwei Bao [a,*], Chuangjiu Li [b], Zhenhua Zhao [a]

[a] Key Laboratory for Mineralogy and Metallogeny, Guangzhou Institute of Geochemistry, Chinese Academy of Sciences, Guangzhou 510640, China
[b] Guangdong Nonferrous Metals Geological Exploration Institution, Guangzhou 510080, China

ARTICLE INFO

Article history:
Received 13 March 2014
Received in revised form 31 March 2015
Accepted 2 April 2015
Available online 3 April 2015

Keywords:
Syenite-related gold deposit
Late-magmatic hydrothermal process
Au-Te association
Dongping
North China Craton

ABSTRACT

The Dongping gold deposit is located at the northern margin of the North China Craton in Hebei Province, China; it is the largest alkaline pluton-related Au deposit in China. The ore deposit is hosted in the 400–386 Ma (LA-ICPMS and SHRIMP zircon U–Pb method) Shuiquangou syenite intrusion, which cuts Archean-aged metamorphic rocks. The ore bodies consist of a set of *en echelon* lenses and veins controlled by shear zones. The ores can be divided into auriferous quartz vein, stockwork, and disseminated ores. Two stages of gold mineralization can be distinguished, the first stage mineralization consists of high grade (>10 g/t) grayish quartz veins enveloped by stockwork and disseminated ores, whereas the second stage mineralization occurs as low grade (<10 g/t) milky white quartz veins. The ores are sulfide-poor and enriched in Te. Gold is mainly present as native gold, calaverite, electrum and petzite.

Studies of fluid inclusions in quartz indicate that the ore-forming fluids have low salinity (0.7–8.1% NaCl equivalent) in the H_2O–CO_2–NaCl system and have homogenization temperatures varying from 310 to 350 °C. The ore-forming fluids have $\delta^{18}O$ values varying from −1.7 to +6.9‰ with an average of 2.9‰ and δD values from −108 to −66.5‰ with an average of −85‰, indicating a magmatic origin with some involvement of meteoric fluid. The ore-forming fluids have initial $^{87}Sr/^{86}Sr_{385Ma}$ ratios of 0.705–0.706 and $^{3}He/^{4}He$ ratios of 0.3 to 5.2 Ra (Ra being the atmospheric ratio of 1.0), indicative of a mantle contribution of the fluids. The ores have bulk $\delta^{34}S$ values varying from −1 to +2‰, similar to those of the host syenites ($\delta^{34}S$ = 1.8–3‰) and the Archean metamorphic rocks ($\delta^{34}S$ = 0.04 to +4.4‰). Lead isotope analyses of sulfides, stock and disseminated ores, quartz veins, fresh host syenites and the Archean metamorphic rocks have a linear correlation of $^{208}Pb/^{206}Pb$ and $^{207}Pb/^{206}Pb$, indicating a genetic link between the gold mineralization and the syenites. Hydrothermal zircons from the high grade ores of the first stage can be distinguished from magmatic zircons based on internal textures on cathodoluminescence images and rare earth element patterns; these zircons have been dated at 389 ± 1.0 to 385 ± 5.7 Ma, whereas those from the second stage low-grade auriferous quartz vein were dated at ~140 Ma (LA-ICPMS and SIM U–Pb methods).

We propose a model for the formation of the Dongping gold deposit involving a late-magmatic hydrothermal process related to a Devonian mantle sourced syenites with a Late Jurassic–Early Cretaceous hydrothermal overprint.

1. Introduction

The association of epithermal and porphyry gold deposits with alkaline igneous rocks has been of interest for nearly a century, especially since the discovery of a few world-class gold deposits such as the Porgera, Emperor, Ladolam and Cripple Creek deposits (Jensen and Barton, 2000; Kelly and Ludington, 2002). The alkaline igneous rocks that are related to the gold deposits are diverse, including kimberlite, lamprophyre, alkali basalt, highly evolved felsic syenite, phonolite, peralkaline granite, rhyolite and trachyte. Among them, gold deposits related to syenitic intrusions are only rarely reported (Robert, 2001; Sillitoe, 2002; Wyman and Kerrich, 1988). The syenite-related gold deposits are generally Te-rich and Cu- and Zn-poor and have an oxidized ore mineral assemblage syngenetic with potassic alteration, and therefore this deposit type was termed an "oxidized intrusion-related gold deposit" (Helt et al., 2014).

Gold deposits related to alkaline magmatism had not been reported in China until the Dongping syenite-related gold (Au) deposit was found in 1985. The Dongping gold deposit is hosted in the Shuiquangou syenite intrusion in the northern margin of the North China Craton. The proven reserve is about 100 t of contained Au (Mao et al., 2003). The discovery of the deposit has triggered further exploration for this type of Au deposit in the North China Craton (Hu et al., 2006a; Nie et al.,

* Corresponding author.
E-mail address: baozw@gig.ac.cn (Z. Bao).

http://dx.doi.org/10.1016/j.oregeorev.2015.04.002
0169-1368/

2004). The Dongping Au deposit has been extensively studied since its discovery. Researchers have debated on the origin of the deposit based on different points of views on the age of gold mineralization and source of ore-forming fluids and Au, e.g., the Archean greenstone type (Li, 1999; Wang et al., 1990; Yin, 1994; Yin and Zhai, 1994); orogenic type (Hart et al., 2002; Mao et al., 2003; Miller et al., 1998); remobilization type (Bao and Zhao, 2006; Mo et al., 1997; Song and Zhao, 1996; Wang et al., 1994); and alkalic porphyry association type (Xiang et al., 1992; Nie, 1998; Nie et al., 2004; Zhang et al., 2005).

This contribution reviews the geological background, ore geology and geochemical characteristics of the Dongping gold deposit. A new model for ore-formation of the deposit is proposed. Our results shed new light on the metallogenesis of the Dongping deposit and the signatures of gold deposits associated with syenite intrusions, which may have implications on the exploration of this type of deposits.

2. Geological background

The Dongping Au deposit is located in the western part of the Yanshan orogen in the northern margin of the North China Craton, ~10 km south of the Shangyi–Chongli–Chicheng thrust fault in Hebei Province (Fig. 1). The fault extends more than 200 km along the latitude of 41°N and is a dextral strike-slip fault that cuts the basement of the North China Craton. The pronounced aeromagnetic and gravity anomalies as well as the Moho depth contour show that it is a mantle-penetrating fault (Fig. 1; Hu and Song, 2002; Ma and Zhao, 1999; Zhang et al., 2007). Other sub-parallel WNW-trending subsidiary dextral shear faults, the Yangmuwa–Mazhangzi and Zhongshangou–Honghuabei–Shangshuiquan faults are situated along the northern and southern margins of the Shuiquangou syenite intrusion, and control the emplacement of the syenitic intrusion and the distribution of the Au mineralization (Jiang et al., 2000; Li et al., 2000a; Lu et al., 1997; Song and Zhao, 1996).

The Sanggan metamorphic complex comprises the basement rocks, and is composed of a suite of Neoarchean amphibolite and granulite, and is exposed to the south of the Shangyi–Chongli–Chicheng fault. The granulite gneiss of the Jiangouhe Formation in the Sanggan metamorphic complex was dated at 2.69 to 2.50 Ga using LA-ICPMS and SHRIMP zircon U–Pb methods (Jiang et al., 2010; Li et al., 2012a; Liu et al., 2007) and is well preserved in this region.

The marble, quartzite, amphibolite and gneiss of the Precambrian to Paleozoic Hongqiyingzi complex outcrops to the north of the Shangyi–Chongli–Chicheng fault (Fig. 1). The Hongqiyingzi complex experienced extensive deformation in the late Paleozoic due to the closure of the Paleo-Asian Ocean between the Siberian and North China Cratons (Wang et al., 2011). The rock types at surface in the mining area also include Mesoproterozoic sedimentary rocks and volcanic-sedimentary rocks of the Early Cretaceous Zhangjiakou Group (Fig. 1).

Magmatism in this region occurred in five stages between the Archean and the Cretaceous. The earliest stage magmatic event

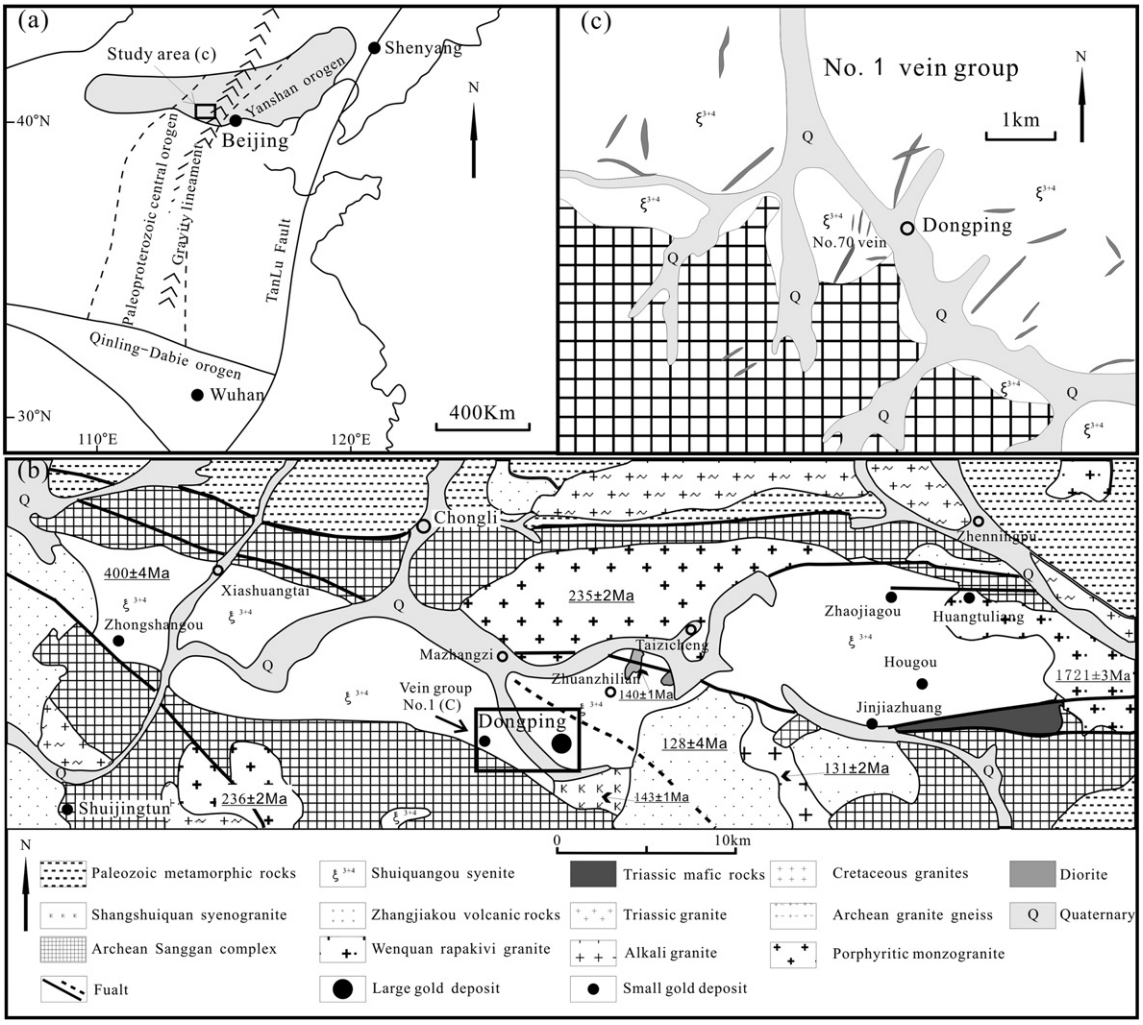

Fig. 1. Geological map showing the distribution of the Shuiquangou syenite intrusion and related gold deposits in the western part of the Yanshan orogen. (a) The location of the study area; (b) the study area; (c) the No.1 vein group of the Dongping gold deposit.

produced the Neoarchean to Paleoproterozoic granodiorite and monzonite (2.54–2.44 Ga, Li et al., 2012a), which were followed by Mesoproterozoic Wenquan rapakivi granite (1721 ± 3 Ma, Liu et al., 2006). A magmatic event in the late Paleozoic formed the Devonian Shuiquangou syenite intrusion (400 ± 3.5 Ma, Bao et al., 2014). Triassic magmatism includes the Guzuizi porphyritic monzogranite (236 ± 2 Ma, Miao et al., 2002), Honghualiang biotite granite (235 ± 2 Ma, Jiang et al., 2007) and Xiaozhangjiakou mafic–ultramafic intrusion (220 ± 5 Ma, Tian et al., 2007). Cretaceous magmatism occurs as the Shangshuiquan alkali granite (142.5 ± 1.3 Ma, Miao et al., 2002), Zhuanzhilian diorite (139.5 ± 0.9 Ma, Jiang et al., 2007), Beizhazi alkali granite (130.5 ± 1.5 Ma; Li and Bao, 2012), and the Zhangjiakou Formation volcanic rocks (127.8 ± 3.9 Ma, Li and Bao, 2012).

2.1. The Devonian Shuiquangou syenite intrusion

The Shuiquangou syenite intrusion, along with a suite of alkaline rocks, mafic–ultramafic intrusions and trachytic rocks, is considered to constitute a linear post-collisional magmatic belt along the northern margin of the North China Craton, which resulted from slab breakoff, the buoyancy-driven detachment of subducted oceanic lithosphere from the light continental lithosphere that follows it during continental collision (Davies and von Blanckenburg, 1995), subsequent to the closure of the Paleo-Asian Ocean (Zhang et al., 2010). The Shuiquangou syenite intrusion crops out in an area of about 350 km^2. It intruded the Neo-Archean Sanggan metamorphic rocks and is locally overlain by the Early Cretaceous volcanic rocks of the Zhangjiakou Formation. The Shuiquangou syenite intrusion is composed of augite hornblende K-feldspar syenite, hornblende syenite, augite syenite, aegirine syenite, K-feldspar syenite, quartz K-feldspar syenite and quartz syenite. Flow structure composed of E–W orientated prismatic hornblende and tablet-like microcline is commonly observed in outcrops at the top and the margins of the intrusion.

The Shuiquangou syenite intrusion is modeled as an upper mantle partial melt that has been contaminated by the lower crust (e.g., Bao et al., 2003; Jiang, 2005; Jiang and Nie, 2003). The syenitic rocks of the Shuiquangou syenite intrusion have very variable rare earth element (REE) concentrations (3 to 83 times that of the chondrite); the augite hornblende K-feldspar syenite in the west contains the highest ∑REE of ~212 ppm and has smooth chondrite-normalized REE pattern with depletion of HREE relative to LREE. In contrast, quartz K-feldspar syenite in the east has the lowest ∑REE of ~8.54 ppm and exhibits obviously tetrad effect (Fig. 2). The "tetrad effect" of REE (La–Lu) results from increased stability at quarter, half, three-quarter, and complete filling of the 4f electron shell. This effect can cause a split of chondrite-normalized REE patterns into four rounded either convex or concave segments called tetrads (first tetrad, La–Ce–Pr–Nd; second tetrad, (Pm)–Sm–Eu–Gd; third tetrad, Gd–Tb–Dy–Ho; fourth tetrad, Er–Tm–Yb–Lu) (Masuda and Ikeuchi, 1979). The tetrad effect was initially observed in patterns of liquid–liquid REE distribution coefficients, and subtle interelement variations resembling this effect have been subsequently documented by various experimental studies and theoretical considerations (Monecke et al., 2002, and reference therein). The REE tetrad effects found in the syenites from the mining area and K-feldspathized and silicified syenites adjacent to the auriferous quartz veins are likely the result of intensive hydrothermal alteration (Bao et al., 1996; Zhao et al., 2010) The host syenite intrusion to the Dongping gold mine has been intensely altered by late-magmatic, high-K and F-rich hydrothermal fluids (Jiang, 2006; Jiang et al., 2003) and experienced silicification and K-feldspathization; euhedral allanite has been replaced by anhedral allanite, and chevkinite-(Ce) replaced by allanite and ilmenite.

The Shuiquangou syenite intrusion has been dated by many different methods. ^{40}Ar–^{39}Ar ages on hornblende (327 ± 9 Ma) and K-feldspar from the syenites (157–177 Ma) are unreliable, given the late-stage hydrothermal and structural disturbance (e.g., Jiang and Nie, 2000; Song and Zhao, 1996). Single zircon U–Pb results ranging from 410.5 ± 1.4 Ma to 1667 ± 11 Ma are also questionable because of the lack of structural studies (Li et al., 1999; Liang et al., 1998). The more recent LA-ICPMS and SHRIMP zircon U–Pb dating show that the Shuiquangou syenite intrusion may have experienced a prolonged history of crystallization, i.e., zircons from the hornblende syenite in the western part, K-feldspar syenite in the middle part, and quartz syenite in the eastern part of the intrusion were dated at 400 ± 3.5 Ma, 390 ± 6 Ma, and 386 ± 6 Ma, respectively (Bao et al., 2014; Miao et al., 2002).

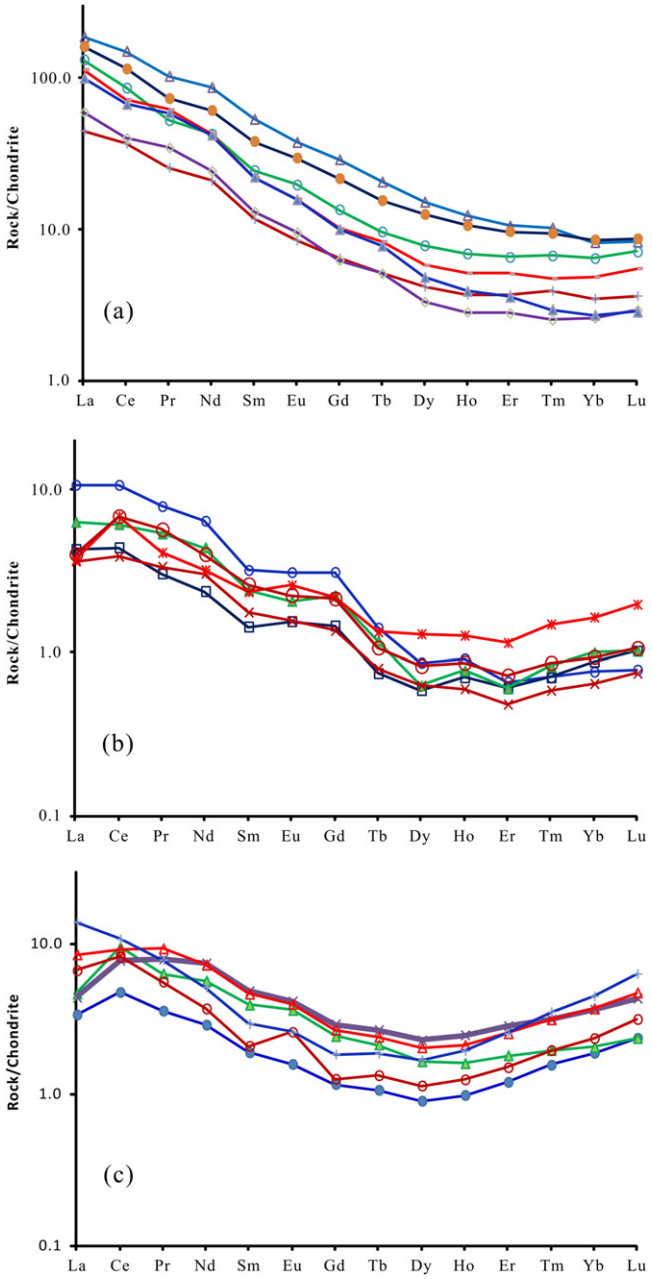

Fig. 2. Chondrite-normalized REE patterns for the augite–hornblende syenites from the southern part of the Shuiquangou syenite intrusion (a); syenites and quartz syenites from the mining area the Dongping gold deposit (b); intensively K-feldspathized and silicified syenites adjacent to the auriferous quartz veins from the 1427 m level of the No.1 vein group (c). REE concentrations of the samples are from Bao et al. (1996), Bao and Zhao (2003), and Zhao et al. (2010). REE normalization values are from Sun and McDonough (1989).

2.2. The Dongping gold deposit

The Dongping gold deposit is located in the middle part of the Shuiquangou syenite intrusion. The gold mineralization is controlled by three stages of fractures (Song and Zhao, 1996; Jiang et al., 2000). The first-stage fractures are oriented in two directions, one group of fracture strikes at 050° and dips NW at an angle of 45°, and the other set of fractures is nearly EW-trending and dips north at an angle of ~60°. Both sets of fractures are filled with barren or weakly gold-mineralized quartz veins. The second-stage shear zones are the major gold-controlling structures; they comprise NNE-trending sinistral and NW-striking dextral shear faults which are en echelon. Major gold ore bodies are hosted in a series of subparallel NNE-striking, en echelon auriferous quartz vein swarms and quartz-K-feldspar veinlets. The third-stage structure is observed locally, comprising NE-striking dextral tensional shear faults. The gold mineralization hosted in the third-stage structure is minor and restricted in distribution to the western part of the ore field.

A total of 69 auriferous veins or vein groups have been identified in the Dongping gold deposit. The quartz veins are enveloped by intensively K-feldspathized and silicified syenite, commonly a few tens of centimeters to a few meters in thickness, and up to 30 m in thickness at depth. The vein group No.1–70, which comprises the main part of the deposit, is more than 1300 m long and has width varying from tens of meters to more than 500 m, with a depth extension of more than 800 m (Fig. 3). Individual ore bodies are 200 to 400 m long, 0.12 to 36 m thick (average of 10.6 m) and have a depth extension of 100 to 600 m. The density of ore vein distribution increases with depth, and the disseminated ores enveloping the veins become the main ore type at depth (Fig. 4).

The Dongping gold deposit has an average gold grade of 6 g/t. The grade of individual ore body is variable from 4.14 to 22.66 g/t (Song and Zhao, 1996). There are three major ore types in the deposit, i.e., auriferous quartz vein in the upper part, quartz stockwork and disseminated ores in the middle part, and disseminated ores in the lower part. The ores contain <3% sulfides. The sulfides mainly comprise pyrite that is commonly replaced by limonite at the shallow part, with minor chalcopyrite, galena, and sphalerite. Specularite, magnetite, bornite, covellite, cerussite and malachite are also observed in the ores. The oxygen fugacity reached the hematite–magnetite oxygen buffer, which is similar to that of porphyry Cu–Au deposits (Sun et al., 2013). Gangue minerals include quartz, microcline and albite, with minor sericite, calcite and barite. Wall rock alteration includes K-feldspathization, albitization, silicification, pyritization, sericitization, chloritization and epidotization.

Native gold makes up >90% of Au in the ores, and is mostly fine-grained and rarely visible in hand specimen. Native gold is commonly cubic or octahedral or vein-, worm-like or spherical in shape. Coarse-grained native gold is associated with quartz, pyrite, galena and chalcopyrite, whereas disseminated, fine-grained native gold is associated with euhedral fine-grained pyrite, galena and calaverite in the late stage quartz veins.

The second major gold carrier is represented by gold and silver telluride, including calaverite, hessite and petzite. Au–Ag-telluride occurs as nanoparticles in As-free pyrite (Ciobanu et al., 2012; Cook et al., 2009a). The ores have an average Te/Au ratio of 0.71, and the Te/Au ratio increases with the grade of Au (Zhang et al., 2001). The Dongping gold deposit was therefore referred to as Au-telluride deposit (e.g., Zhang and Mao, 1995). The telluride minerals have a grain size ranging from 10 to 47 μm, and are associated with native gold and chalcopyrite, or

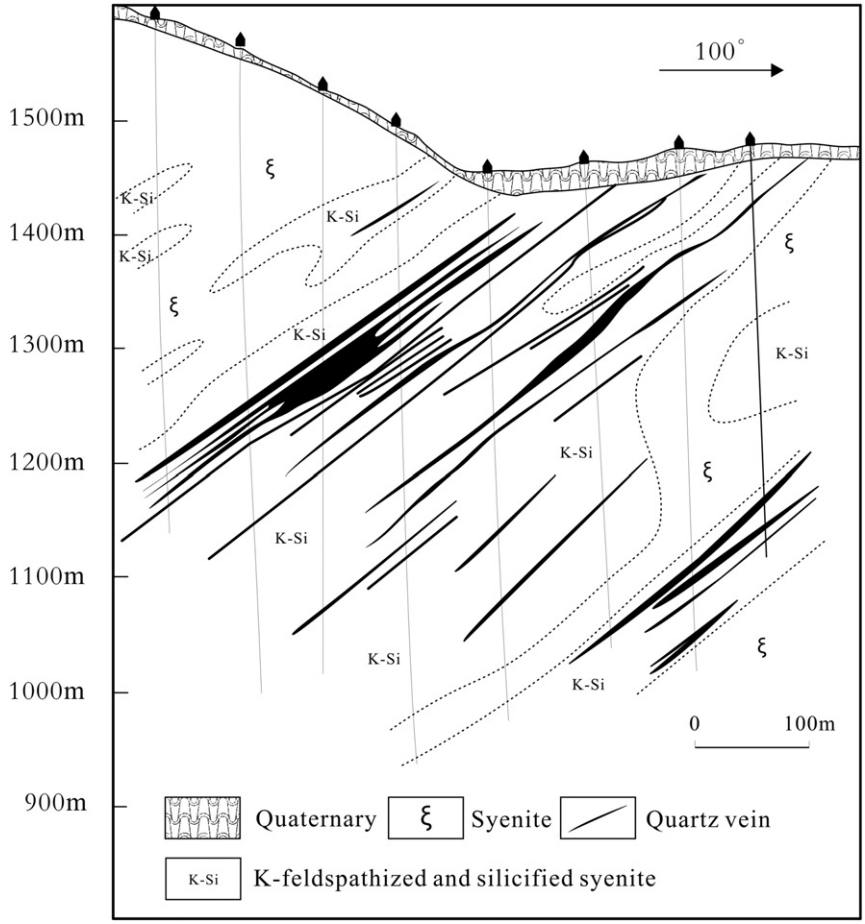

Fig. 3. A cross section of the Dongping gold deposit along the No. 15 exploration line.

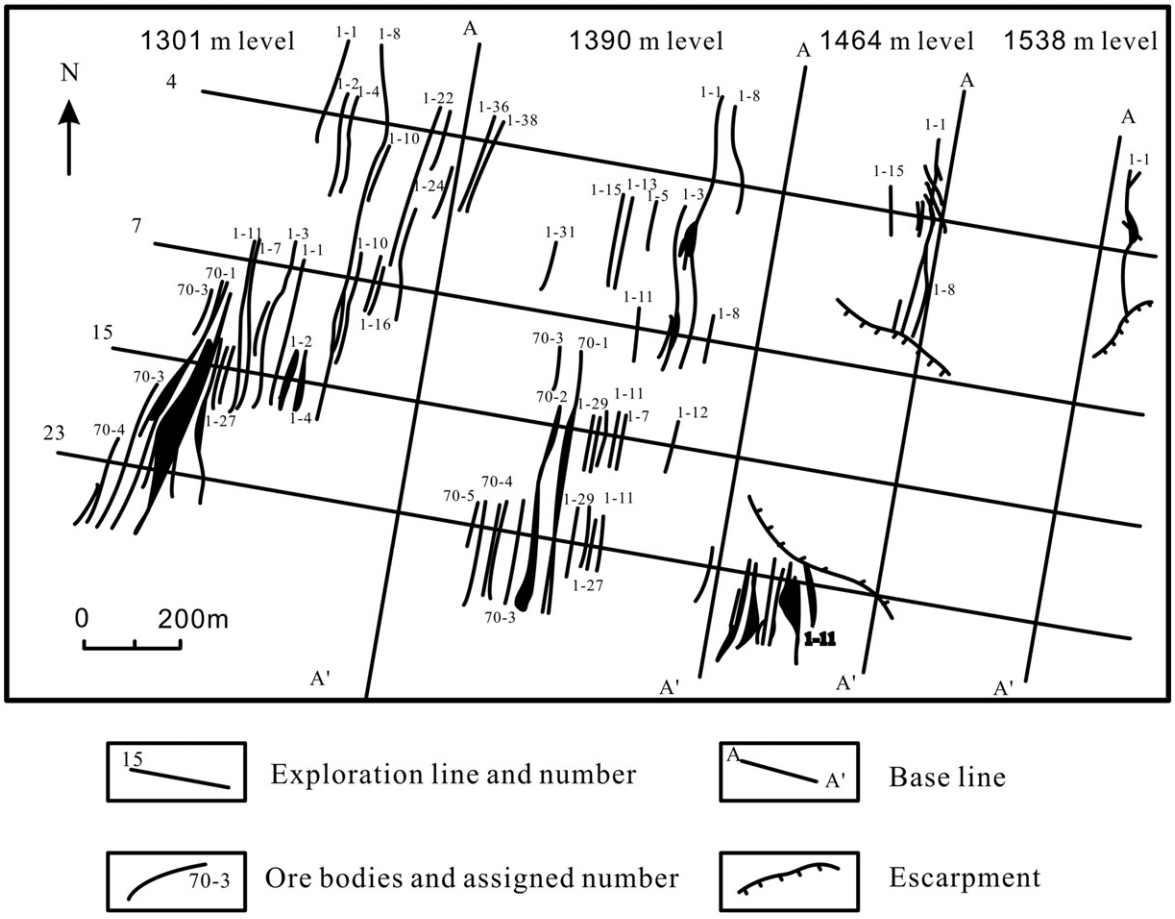

Fig. 4. A plan view of No.1–70 groups of the veins in the Dongping gold deposit, within which all the veins at four levels are projected onto one surface and aligned with the exploration line A–A′.

as inclusions and fissure-fillings in pyrite, galena, sphalerite and quartz (Zhang et al., 2002a). The oxidation and dissolution of the tellurides resulted in the formation of tellurium oxysalts and secondary native gold (Li et al., 2001; Zhang et al., 2002b). Replacement of native gold by the secondary native gold (>98% Au) or Au-bearing Pb, Zn, and Te minerals is locally observed under microscopy. A few newly described tellurite minerals such as zincospiroffite [$Zn_2Te_3O_8$] have been discovered in the deposit (Tian and Li, 1995; Wang and Meng, 2000; Zhang et al., 2000, 2004).

The cross-cutting relationships of ore veins with the different mineral assemblages show that there are two stages of gold mineralization at the Dongping gold deposit. These include: 1. the early stage high grade grayish auriferous quartz-K-feldspar veins (>10 g/t) along with the enveloping stockworks and disseminated ores and 2. the late stage of low grade white auriferous quartz veins (<10 g/t) and auriferous quartz-polymetallic sulfide veins that crosscut the early stage quartz veins and stockworks. Calcite–pyrite veins are rarely visible in hand specimen and are only observed as fine veinlets in thin sections, occurring as fracture fillings.

3. Geochemical constraints on the ore-forming processes

3.1. Fluid inclusion data

Three types of fluid inclusions have been identified in the auriferous quartz veins based on the fluid inclusion relationships and their chemical compositions at room temperature (Fan et al., 2001; Mao et al., 2003; Mao and Li, 2001). These types are: (1) gas inclusion (V-type), containing more than 50 v/v% (percent by volume) vapor phase. The V-type inclusions occur in isolation, mostly as negative crystal or ellipsoidal shape with diameters of 5 to 10 μm and are primary. (2) Gas-liquid inclusion (V–L type), comprising 10 to 50 v/v% vapor phase. The V–L type inclusions commonly occur in clusters or healed fractures and show ellipsoidal or negative crystal shapes with diameters of 2 to 15 μm. (3) Liquid inclusions (L-type), containing less than 10 v/v% vapor phase, with an ellipsoidal and irregular shape, and diameters of less than 7 μm. The L-type inclusions occur in healed fractures and cut V- and V–L-type inclusions and they are secondary in origin. Primary CO_2-rich inclusion (V-type) and vapor-rich liquid inclusion (V–L-type) have homogenization temperatures of 372–306 °C and 342–267 °C and salinities of 3.7–1.0 and 1.9–0.8 wt.% NaCl equivalent, respectively (Fan et al., 2001). The trapping pressures for V-type inclusions are estimated to be 0.4–1.6 kbar (Fan et al., 2001; Mao et al., 2003; Zhang et al., 2012). The ore-forming fluid was a low-salinity H_2O–CO_2–NaCl system, which is typical for mesothermal gold deposit (Wilkinson, 2001). From deep to shallow part of ore veins, homogenization temperature of inclusions decreases and the salinity of ore fluids changes from 1.9 to 0.8 wt.% NaCl equivalent, which may be due to dilution by meteoric water and/or boiling (Fan et al., 2001; Wilkinson, 2001). Fluid immiscibility was observed in inclusions in the middle parts of No.1 ore zone, which might have been resulted from changes of temperature and pressure. We believe that fluid immiscibility may be the prime depositional mechanism for gold in the auriferous quartz veins (Fan et al., 2001).

The ore-forming fluids have $\delta^{18}O$ values calculated using the quartz–water fractionation equation of Clayton (1972) ranging from −1.7 to +6.9‰ (average 2.9‰) and δD values from −108 to −66.5‰ (average −85‰), indicating that the fluids may have been derived from magmatic water with the involvement of meteoric waters during the

Table 1
Oxygen and hydrogen isotope compositions of quartz from the Dongping gold deposit.

Sample number	$\delta^{18}O_{Mineral}$	$\delta^{18}O_{H_2O}$	$\delta D_{fluid\ inclusion}$	Refs.
D91-01	9.1	2.5	−83.0	Lu (1991)[a]
D91-02	12.0	5.3	−81.0	Lu (1991)[a]
D92-06	11.6	4.5	−81.0	Lu (1991)[a]
D91-03	8.2	−1.7	−81.0	Lu (1991)[a]
D91-04	11.3	−0.3	−85.0	Lu (1991)[a]
D95-11	13.1	1.5	−79.3	Nie (1998)
D95-12	11.4	1.4	−93.1	Nie (1998)
D95-07	13.0	5.8	−73.1	Nie (1998)
D95-08	13.5	6.9	−76.2	Nie (1998)
D95-09	12.3	6.0	−73.2	Nie (1998)
D95-10	12.3	5.9	−79.3	Nie (1998)
D92-02	11.8	4.0	−91.2	Wang et al. (1992)
D92-01	6.80	−1.5	−89.2	Wang et al. (1992)
D92-03	10.5	1.10	−89.3	Wang et al. (1992)
D92-04	6.80	−1.70	−66.5	Wang et al. (1992)
D92-05	11.2	2.20	−101	Wang et al. (1992)
DP-39	10.7	2.44	−108	Fan et al. (2001)
DP-53	11.5	4.05	−108	Fan et al. (2001)
DP-51	10.8	3.55	−91.0	Fan et al. (2001)
DP-63	10.5	3.59	−89.4	Fan et al. (2001)
DP-32	10.7	3.99	−84.7	Fan et al. (2001)
DP-19	11.0	3.35	−70.8	Fan et al. (2001)
DP-15	10.8	3.15	−85.9	Fan et al. (2001)

[a] Lu, D.L., 1991. Ore-control structures and metallogenesis of the Dongping gold deposit. Geological report.

process of ore-formation (Fan et al., 2001; Nie, 1998; Wang, 1992) (Table 1 and Fig. 5). In the No.1 group of veins, the δD values of fluids decrease obviously from the depth upwards, indicating that there was an incremental input of meteoric water to the primary magmatic fluid (Fan et al., 2001).

The ore-forming fluids in six quartz samples from the auriferous quartz veins contain 0.0206–0.5901 ppm Rb and 0.4941–3.342 ppm Sr, and have $^{87}Sr/^{86}Sr$ ratios ranging from 0.706 to 0.708 (Mo et al., 1997). The initial $^{87}Sr/^{86}Sr$ ratios (at 385 Ma) of the ore-forming fluids

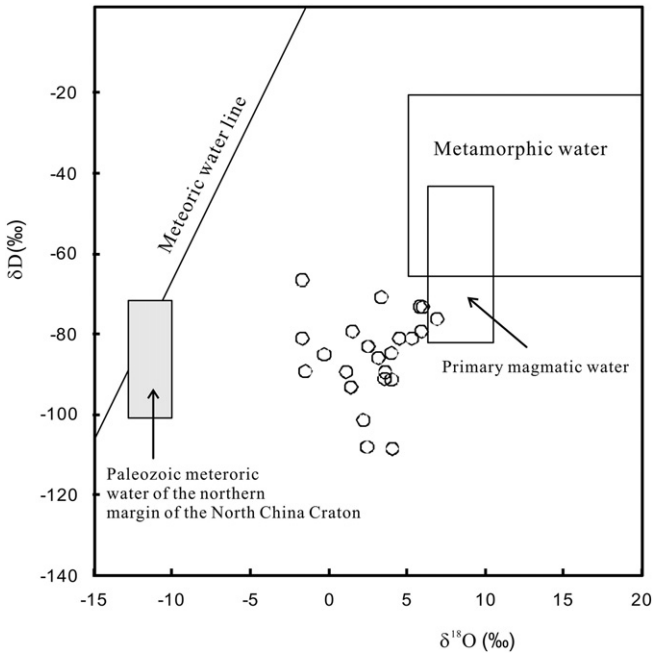

Fig. 5. Hydrogen and oxygen isotopic compositions of the ore fluids in the Dongping gold deposit. Note: $\delta^{18}O$ values of the ore-forming fluids are calculated using the quartz–water fractionation equation of Clayton (1972) ($1000\ln\alpha_{quartz-water} = 3.38 \times 10^6\ T^{-2} - 3.40$) based on the results of oxygen isotopic compositions of representative quartz from the auriferous quartz veins and the homogenization temperatures of the fluid inclusions. Data sources: Fan et al. (2001); Lu (1991); Nie (1998); Wang (1992). Reference fields are after Taylor (1997)

vary from 0.705 to 0.706, almost identical to that of the host syenitic plutons ($^{87}Sr/^{86}Sr_{385Ma} \sim 0.705$, Bao et al., 1996, Table 2). Such similarity indicates a genetic link between the ore-forming fluids and the host syenite intrusion (Mo et al., 1997).

The fluid inclusions in the pyrite from the ore veins have $^3He/^4He$ ratios ranging from 0.3 to 5.2 Ra (Ra being the atmospheric ratio of 1.0), which are much higher than that of the crustal values and indicate a mantle source for the fluids (Mao et al., 2003).

3.2. The source of gold

Pb isotope data for the sulfides, disseminated ores and auriferous quartz veins plot along a co-linear array with the K-feldspar, host syenitic plutons and the Archean Sanggan metamorphic complex on the plots of $^{207}Pb/^{204}Pb$ versus $^{206}Pb/^{204}Pb$, $^{208}Pb/^{204}Pb$ versus $^{206}Pb/^{204}Pb$ and $^{208}Pb/^{206}Pb$ versus $^{207}Pb/^{206}Pb$ (Fig. 6; Bao et al., 2000; Nie, 1998; Wu, 2009). This indicates that mixing of Pb sources may have been involved in the hydrothermal ore-forming processes. The sulfides, disseminated ores and auriferous quartz veins contain more radiogenic Pb, which may be attributed to the preferential scavenging of radiogenic Pb that results in the more radiogenic leachate fraction than whole rock lead during hydrothermal processes (Davis and Krogh, 2000; Macfarlane and Petersen, 1990; Nimis et al., 2012). Given the similarity of the Pb isotopic composition of the disseminated ores and the host syenite intrusion, the majority of the ore-forming elements may have been sourced from the syenites. The Pb isotope composition of the Archean metamorphic rocks is different when compared to the ores, and the trend shifts away from the field of the ores and syenites even though the data fall on the same array. We, therefore, suggest that the Archean Sanggan metamorphic complex is unlikely the major source of ore metals for the gold mineralization in the Dongping deposit.

The sulfides from the Dongping deposit and the other gold deposits related to the Shuiquangou syenite intrusion have variable $\delta^{34}S$ values, which may have resulted from different sulfur source and/or distinct oxygen fugacity (Fig. 7, Table 4). It is recognized that the $\delta^{34}S$ values of hydrothermal sulfide minerals are controlled by many factors (Ohmoto, 1972): (a) temperature; (b) the isotopic composition of sulfur in the ore fluid ($\delta^{34}S_{\sum S}$); and (c) the ratio of SO_4^{2-}/H_2S in the solution which, in turn, is controlled by the temperature, pH, and f_{O2}, the hydrothermal fluid. The $\delta^{34}S$ values of the sulfides from the Dongping deposit show $\delta^{34}S_{pyrite} > \delta^{34}S_{sphalerite} > \delta^{34}S_{galena}$ (Song and Zhao, 1996), which is consistent with the trend of equilibrium sulfur isotopic fractionation (Fig. 7a, b, c, d; Ohmoto and Rye, 1979). The presence of magnetite and specularite in the ores demonstrates that the Dongping gold deposit was formed under oxidized condition, and the bulk $\delta^{34}S$ value was estimated to be −1 to +2‰ (Ohmoto, 1972). The bulk $\delta^{34}S$ value of the ore-forming fluids is quite similar to that of the magmatic pyrite from the Shuiquangou syenites ($\delta^{34}S = +1.8$ to +3‰, Nie, 1998) and rocks of the Archean Sanggan metamorphic complex ($\delta^{34}S = -0.04$ to +4.4‰, Wang et al., 1990). Therefore, the Shuiquangou syenites may have been the principal sulfur source for the ore-forming fluids but a contribution of sulfur from the Archean metamorphic rocks cannot be excluded.

3.3. Age of gold mineralization

Early isotopic dating yielded ages of 350 to 103 Ma, most of which are by the $^{39}Ar/^{40}Ar$ method (Table 5; Hart et al., 2002; Jiang and Nie, 2000; Lu et al., 1993). The diversity in ore-formation ages led to much controversy over metallogenic models (e.g., Hu and Luo, 1994; Jiang and Nie, 2000; Li et al., 1998, 2010; Mao et al., 2003; Nie, 1998; Wang, 1992; Xu et al., 2002).

Previous work on the $^{39}Ar/^{40}Ar$ ages of the hydrothermal K-feldspar, quartz, and sericite yielded ages between 289 and 153 Ma (e.g., Hart et al., 2002; Jiang and Nie, 2000). It is likely that these ages recorded the time of the Ar gain and/or loss during multistage hydrothermal

Table 2
Rb–Sr isotope compositions of the fluid inclusions from the auriferous quartz veins and the syenite complex.

Sample no.	Sample type	Rb (ppm)	Sr (ppm)	$^{87}Rb/^{86}Sr$	$^{87}Sr/^{86}Sr$	$^{87}Sr/^{86}Sr_{385Ma}$
D39	Fluid inclusions	0.2398	0.4941	1.3991	0.70825 ± 0.00008	0.7006
D61	Fluid inclusions	0.0305	0.6950	0.1263	0.70640 ± 0.00001	0.7057
D77	Fluid inclusions	0.0206	0.9732	0.0609	0.70632 ± 0.00002	0.7060
D146	Fluid inclusions	0.0619	0.6876	0.2596	0.70650 ± 0.00003	0.7051
D185	Fluid inclusions	0.3500	3.342	0.3019	0.70670 ± 0.00010	0.7050
D174	Fluid inclusions	0.5901	1.654	1.0285	0.70845 ± 0.00002	0.7028
DP92-93	Augite hornblende syenite	73.65	1404	0.1505	0.70571 ± 0.00001	0.7049
DP92-98	Augite hornblende syenite	112.8	1232	0.2050	0.70685 ± 0.00001	0.7057
DP92-122	Quartz syenite	75.69	673.6	0.3252	0.70781 ± 0.00002	0.7060
DP92-160	Augite syenite	69.54	1051	0.1915	0.70674 ± 0.00001	0.7057
DP92-162	Quartz syenite	53.38	914.1	0.1690	0.70616 ± 0.00001	0.7052
DP92-169	Hornblende syenite	68.10	134.0	0.1470	0.70581 ± 0.00001	0.7050
DP-4	Quartz syenite	19.09	127.4	0.1537	0.70609 ± 0.00001	0.7052
DP-5	Quartz syenite	13.44	1.996	0.5764	0.70770 ± 0.00003	0.7045
DP-6	Quartz syenite	23.51	155.8	0.1597	0.70580 ± 0.00005	0.7049
DP-7	Quartz syenite	20.40	677.1	0.0875	0.70559 ± 0.00005	0.7051
DP-8	Quartz syenite	18.15	120.3	0.1546	0.70647 ± 0.00003	0.7056
DP-9	Quartz syenite	3.446	28.83	0.1233	0.70594 ± 0.00002	0.7053
DP-10	Quartz syenite	14.28	112.2	0.3597	0.70601 ± 0.00006	0.7040
DP-11	Syenite	15.67	196.8	0.8160	0.70539 ± 0.00003	0.7009
DP-12	Syenite	20.03	166.2	0.1235	0.70587 ± 0.00004	0.7052
DP-13	Syenite	18.35	136.2	0.1378	0.70599 ± 0.00002	0.7052
DP-14	Syenite	17.40	155.4	0.1148	0.70579 ± 0.00005	0.7052
DP-15	Syenite	18.07	222.6	0.0832	0.70563 ± 0.00005	0.7052

Note: Rb–Sr isotope results for the fluid inclusions in the quartz from the auriferous quartz vein were analyzed by the Yichang Institute of Geology and Mineral Resources, Chinese Academy of Geological Sciences using MAT-261, details were described in Mo et al. (1997). Rb–Sr isotope results were analyzed by the Institute of Geology and Geophysics, Chinese Academy of Sciences using MAT-262.
$^{87}Sr/^{86}Sr_{385Ma}$ represents back calculated $^{87}Sr/^{86}Sr$ ratios of the samples at 385 Ma.

activities and/or mixing processes throughout the multistage hydrothermal events (Villa and Williams, 2013). The argon ages cannot be related to any specific tectonomagmatic event in the study area (Fig. 8; Jiang et al., 2007; Li and Bao, 2012; Miao et al., 2002).

Hydrothermal zircons from high-grade auriferous quartz vein and disseminated ores in the Dongping gold deposit exhibit internal structures and REE patterns that are different from magmatic zircon. The hydrothermal zircons were dated at ~385 Ma by LA-ICPMS and SIMS U–Pb, indicating that they formed during the main stage of gold mineralization in the Devonian (Bao et al., 2014). The hydrothermal zircons from the low-grade auriferous quartz vein of the Dongping gold deposit have been dated at 147.8 ± 2.3 Ma (SIMS) and 140.3 ± 1.4 Ma (LA-ICPMS) (Bao et al., 2014; Li et al., 2010); these ages are attributed to a Late Jurassic–Early Cretaceous hydrothermal overprint caused by the intrusion of the Shangshuiquan granite and the Zhuanzhilian diorite (Bao et al., 2014). On this basis, we suggest that the Dongping gold deposit was mainly formed in the Devonian and overprinted by Late Jurassic–Early Cretaceous hydrothermal activity (Fig. 8).

4. Metallogeny of the Dongping gold deposit

Four models have been proposed for the origin of the Dongping deposit, viz: 1. Greenstone-type (Li et al., 1999; Wang et al., 1990); 2. Orogenic-type (Hart et al., 2002; Yang et al., 2003); 3. Remobilization-type (Song and Zhao, 1996; Wang et al., 1994); and 4. Alkalic porphyry association type (Nie et al., 2004; Xiang et al., 1992).

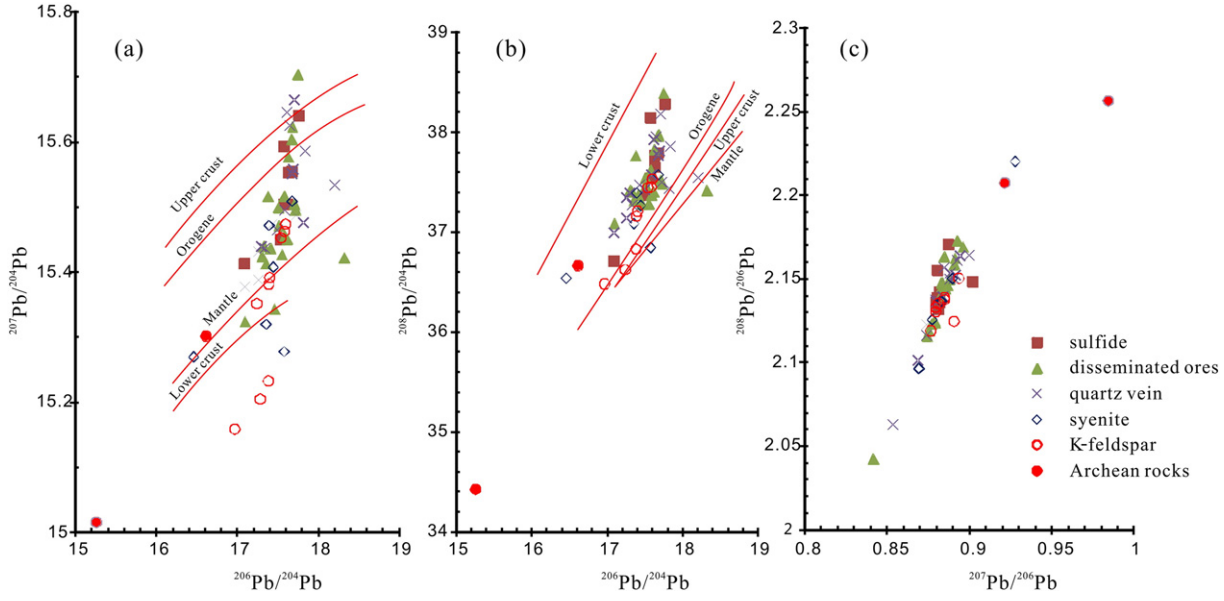

Fig. 6. Lead isotopic compositions of the sulfides, auriferous quartz veins and disseminated ores of the Dongping gold deposit, and the host syenites and Archean Sanggan metamorphic complex. Evolution curves in (a) and (b) according to the plumbotectonic model of Zartman and Haines (1988).

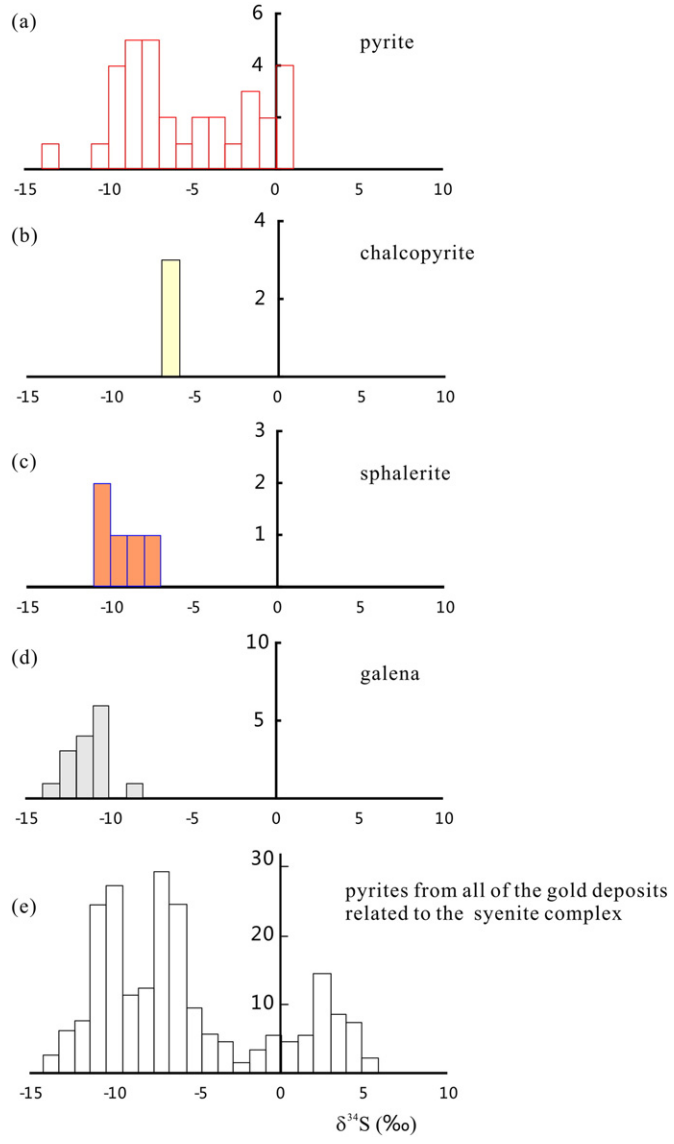

Fig. 7. Histogram of $\delta^{34}S$ value of the sulfides from the Dongping gold deposit and all the other gold deposits related to the Shuiquangou syenite intrusion. (a), (b), (c), and (d) show $\delta^{34}S$ values of sulfide minerals from the Dongping gold deposit; (e) shows $\delta^{34}S$ values of pyrite from the Dongping, Hougou, Jinjiazhuang, Zhongshangou, Zhangquanzhuang, Huangtuliang, and Shijingtun gold deposits associated with the Shuiquangou syenite intrusion.
Data are from Jiang and Nie (1998), Li et al. (2000b), Song and Zhao (1996), Wang et al. (1990), Xing et al. (2011), and Yin (1994).

The Dongping deposit and many other gold deposits in the western part of the Yanshan orogen are spatially associated with the Archean Sanggan metamorphic complex which contains elevated abundances of gold (1.1–9.3 ppb, average 8 ppb; Yin, 1994) relative to bulk crustal crust (1.3 ppb; Rudnick and Gao, 2003). Some researchers have postulated that these gold deposits are of the greenstone-type (Li, 1999; Li et al., 1999; Wang et al., 1990; Yin, 1994; Yin and Zhai, 1994). However, this hypothesis is contradicted with the fact that all the gold deposits in the Northwest Hebei Province are located inside or adjacent to the Shuiquangou syenite intrusion.

The Dongping and other gold deposits in Southwestern Hebei Province have features similar to those of orogenic type gold deposits, such as the sulfide-poor, Te-rich ore mineral assemblages, stockwork ore structures, and low salinity and CO_2-rich ore-forming fluids (Hart et al., 2002). Some researchers have proposed an orogenic model for the Dongping deposit and other gold deposits in the North China Craton. They recognized the spatial coincidence with Archean uplift and have argued that the structures associated with basement uplift were key to localizing magmatism and mineralization, and that reactivation of these structures ensured their role in focusing fluids. They suggested that the lithospheric thinning in the Mesozoic resulted in replacement by hot fertile asthenosphere that resulted in a significant increase in the crustal thermal gradient, uplift, rifting, and subsequent subsidence is one possible mechanism for the formation and localization of the gold deposits in the North China Craton (Hart et al., 2002; Mao et al., 2003; Miller et al., 1998; Zhai et al., 2002; Yang et al., 2003). An orogenic model has been proposed for the ~125 Ma extensive gold mineralization in eastern Shandong province in East China which is related to the coeval lithospheric thinning, asthenospheric upwelling, and paleo-Pacific plate subduction (e.g., Fan et al., 2003; Goldfarb and Santosh, 2014; Hu et al., 2006b; Sun et al., 2007; Yang et al., 2003). Goldfarb and Santosh (2014) proposed that the ore fluids were produced directly by the metamorphism of oceanic lithosphere and overlying sediment on the subducting paleo-Pacific slab, or by devolatilization of an enriched mantle wedge above the slab. Both the sulfur and gold could be sourced from either the oceanic sediments or the serpentinized mantle. Orogenic gold deposits are often associated with greenschist-facies metamorphic rocks (e.g., Goldfarb et al., 2001). The ore-forming ages of the Dongping deposit and other gold deposits in Northwestern Hebei Province are post-date the age of metamorphism of the Archean Sanggan metamorphic complex (e.g., Chen et al., 2006; Hu and Song, 2002; Jiang et al., 2010; Li et al., 2012a). A contribution of metamorphic fluid to the gold mineralization may be insignificant because the Precambrian source rocks had lost most of their volatiles more prior to the formation of the gold mineralization. The commonly meters to tens of meters of halo of K-feldspathization enveloping the ore veins in the Dongping gold deposit are consistent with the development of late-magmatic hydrothermal alteration of the Shuiquangou syenites. Moreover, the extensional tectonic inversion in the North China Craton, which was considered as key event controlling the gold mineralization, took place at 130–110 Ma (Zhai and Santosh, 2011, 2013), which significantly postdated the gold mineralization of the Dongping gold deposit.

Based on similar Pb and S isotopic compositions of the ores and syenites as well as the contrasting ages of mineralization and the Shuiquangou syenite intrusion, some researchers suggested that the hydrothermal fluids were derived from the Late Jurassic–Early Cretaceous granites and leached the gold in the syenites (Song and Zhao, 1996). The Shuiquangou syenites may have been a major contributor of metals in the formation of the gold mineralization; this is supported by the similarity of S, Pb, and silicon isotopic compositions between the ores and the host syenites (e.g., Bao and Zhao, 2006; Mo et al., 1997; Song and Zhao, 1996; Wang et al., 1994). The published $^{39}Ar/^{40}Ar$ ages of K-feldspars and sericites from the ores (153–187 Ma) are substantially younger than that of the Devonian Shuiquangou syenite intrusion. It was thus proposed that the metals were derived from leaching of the Shuiquangou syenites by the circulating hydrothermal fluids related to the development of Late Jurassic–Early Cretaceous granitic intrusions (Bao and Zhao, 2006; Mo et al., 1997; Song and Zhao, 1996). However, the Ar–Ar ages for the hydrothermal gold mineralization cannot be correlated with any specific tectonomagmatic event in the study area and these data are inconsistent with the more reliable U–Pb ages obtained on hydrothermal zircons from the ores (Bao et al., 2014).

A model linking gold mineralization to alkalic magmatism has been proposed by some geologists based on the ore-metal association (they are similar to those of epithermal Au deposits associated with alkaline magmatic rocks), and based on the close spatial relationship of the gold mineralization with the syenite intrusion. Moreover, S and Pb isotope data for the ore-associated minerals support this hypothesis (Table 3, 4) (Xiang et al., 1992; Nie, 1998; Nie et al., 2004; Zhang et al., 2005).

Table 3
Lead isotope compositions of sulfides, ores, and wall rocks from the Dongping area.

Sample	Occurrence	Altitude (m)	Mineral	$^{206}Pb/^{204}Pb$	$^{207}Pb/^{204}Pb$	$^{208}Pb/^{204}Pb$
DP16	Dongping YD7	1620	Galena	17.625	15.505	37.649
89-178	Dongping	1548	Galena	17.630	15.553	37.770
89-189	Dongping	1503	Galena	17.577	15.505	37.540
89-195	Dongping	1464	Galena	17.672	15.555	37.791
DP90①	Dongping	Qtz vein	Galena	17.763	15.641	38.281
DP91①	Dongping	Qtz vein	Galena	17.575	15.593	38.144
90-74	Hougou	1280	Galena	17.145	15.112	36.468
90-67	Hougou	1280	Galena	17.325	15.279	36.908
DP96①	Dongping	Qtz vein	Pyrite	17.533	15.451	37.375
DP97①	Dongping	Qtz vein	Pyrite	17.088	15.413	36.713
Zzs-7②	Zhongshangou	Qtz vein	Pyrite	17.364	15.458	37.384
Zzs-8②	Zhongshangou	Qtz vein	Pyrite	17.292	15.440	37.339
Zzs-13②	Zhongshangou	Qtz vein	Pyrite	17.438	15.469	37.428
DP92-251	Dongping YD6	1620	Ore	17.682	15.623	37.974
DP92-269	Dongping YD3	1584	Ore	17.329	15.440	37.405
DP-17	Dongping YD3	1584	Ore	17.747	15.704	38.389
DP92-227	Dongping	1538	Ore	17.630	15.577	37.823
DP92-230	Dongping	1503	Ore	17.517	15.471	37.460
DP18	Dongping	1503	Ore	17.673	15.604	37.959
DP92-273	Dongping	1464	Ore	17.579	15.517	37.622
B-1	Dongping	1427	Ore	17.413	15.436	37.374
B4	Dongping	1427	Ore	17.553	15.427	37.282
B6	Dongping	1427	Ore	17.506	15.500	37.540
DP92-70-1	Zhongshangou	1330	Ore	18.321	15.422	37.413
DP92-70-3	Zhongshangou	1330	Ore	17.356	15.413	37.314
DP92-70-5	Zhongshangou	1330	Ore	17.303	15.424	37.413
DP92-70-7	Zhongshangou	1330	Ore	17.379	15.517	37.764
DP92-70-9	Zhongshangou	1330	Ore	17.096	15.324	37.084
DP79-1	Dongping	1584	Ore	17.718	15.496	37.486
DP79-2	Dongping	1584	Ore	17.587	15.456	37.368
DP97-5	Dongping	1584	ore	17.615	15.451	37.403
DP97-4	Dongping	1584	ore	17.709	15.504	37.522
DP97-7	Dongping	1538	Ore	17.459	15.343	37.283
DP79-3	Dongping	1538	Qtz vein	17.722	15.488	37.502
DP97-6	Dongping	1538	Qtz vein	17.704	15.665	38.184
DP97-16	Dongping #70	1344	Qtz vein	17.642	15.626	37.955
DP97-32	Dongping #70	1390	Qtz vein	17.428	15.474	37.469
DP97-39	Dongping #4	1740	Qtz vein	17.677	15.552	37.765
DP97-41	Dongping #4	1710	Qtz vein	17.582	15.496	37.572
DP97-42	Dongping #4	1690	Qtz vein	17.836	15.586	37.862
DP97-43	Dongping #4	1675	Qtz vein	17.299	15.440	37.389
DP97-44	Dongping #4	1640	Qtz vein	17.692	15.559	37.812
DP97-46	Dongping #1	1700	Qtz vein	17.818	15.477	37.442
DP97-56	Dongping #2	1735	Qtz vein	17.494	15.465	37.425
DP97-57	Dongping #2	1700	Qtz vein	18.200	15.534	37.547
HT-62	Hetugou	1414	Qtz vein	17.093	15.378	36.994
HT-64	Hetugou	1425	Qtz vein	17.259	15.388	37.146
HT-65	Hetugou	1431	Qtz vein	17.611	15.646	37.926
HT-66	Hetugou	1445	Qtz vein	17.333	15.437	37.273
HT-67	Hetugou	1457	Qtz vein	17.259	15.432	37.348
B-8	Dongping	1427	Syenite	17.676	15.509	37.573
89-27	Yingpandi		Syenite	16.457	15.270	36.539
90-161	Dongping		Syenite	17.390	15.472	37.393
DP238	Dongping		Syenite	17.443	15.408	37.266
DP23①	Dongping		Syenite	17.576	15.278	36.847
90-61	Hougou		Syenite	17.354	15.320	37.084
D159	Dongping #1	1427	Kfs	17.537	15.453	37.447
D173	Dongping #1	1390	Kfs	17.595	15.474	37.533
D129	Dongping #1	1464	Kfs	17.580	15.463	37.452
DP20①	Dongping		Kfs	17.398	15.392	37.211
DP21①	Dongping		Kfs	16.965	15.159	36.482
DP19①	Dongping		Kfs	17.386	15.382	37.163
DP93①	Dongping		Kfs	17.238	15.352	36.625
DP94①	Dongping		Kfs	17.381	15.233	36.831
DP25	Dongping	Archean granulite		16.609	15.302	36.665
DP-26	Dongping	Archean granulite		15.255	15.016	34.425

Note: The samples were analyzed at the State Key Laboratory of Isotope Geochemistry using VG-354 and the details were described in Bao et al. (2000). Data marked ① are from Nie (1998); ② from Wu (2009).
Qtz vein = auriferous quartz vein; Kfs = K-feldspar.

As discussed above, the hydrothermal zircons from the high-grade auriferous quartz veins and disseminated ores have been dated at ~385 Ma, which is immediately after the emplacement of the Shuiquangou syenite intrusion (Bao et al., 2014). The hydrothermal zircon grains from the low grade auriferous quartz vein, which crosscut the early stage high-grade ore veins, have been dated at ~140 Ma, indicating the Late Jurassic–Early Cretaceous hydrothermal overprint (Bao et al., 2014; Li et al., 2010, 2012b).

Table 4
Sulfur isotope composition of the sulfides from the Dongping gold deposit.

Sample no.	Mineral	$\delta^{34}S_{CDT}$ (‰)	Sample no.	Mineral	$\delta^{34}S_{CDT}$ (‰)
D-01	Pyrite	−0.8	A-97	Pyrite	−7.3
D-05	Pyrite	−3.2	A-98	Pyrite	−7.5
D-08	Pyrite	0.5	A-99	Pyrite	−7.4
D-10	Pyrite	−3.7	D-07	Chalcopyrite	−6.7
D-14	Pyrite	−5.3	D-13	Chalcopyrite	−6.7
D-16	Pyrite	−9.5	D-24	Chalcopyrite	−6.9
D-19	Pyrite	−7.8	D-02	Galena	−13.6
D-20	Pyrite	−8.7	D-04	Galena	−11.4
D-22	Pyrite	−7.1	D-09	Galena	−10.4
D-25	Pyrite	−6.9	D-11	Galena	−10.6
D-27	Pyrite	−7.1	D-15	Galena	−12.2
D-28	Pyrite	−6.7	D-17	Galena	−12.5
D-30	Pyrite	0.4	D-21	Galena	−10.5
D-32	Pyrite	0.5	D-26	Galena	−11.7
D-33	Pyrite	−0.3	D-29	Galena	−11.6
D-34	Pyrite	−1.3	D-31	Galena	−10.1
D-35	Pyrite	−2.5	D-33	Galena	−8.2
D-36	Pyrite	−1.7	D-35	Galena	−12.3
D-37	Pyrite	−1.4	D-37	Galena	−10.9
D-38	Pyrite	−4.3	D-40	Galena	−10.2
D-39	Pyrite	−4.2	D-23	Galena	−11.4
DP03	Pyrite	−9.3	D-03	Sphalerite	−10.3
DP06	Pyrite	−9.8	D-12	Sphalerite	−7.8
DP12	Pyrite	−8.9	D-18	Sphalerite	−9.3
DP14-1	Pyrite	−10.3	D-6	Sphalerite	−7.8
CD10	Pyrite	−9.8			

Note: Data are from Song and Zhao (1996) and the results of samples A-97, -98, and -99 are from Wang et al. (1990).

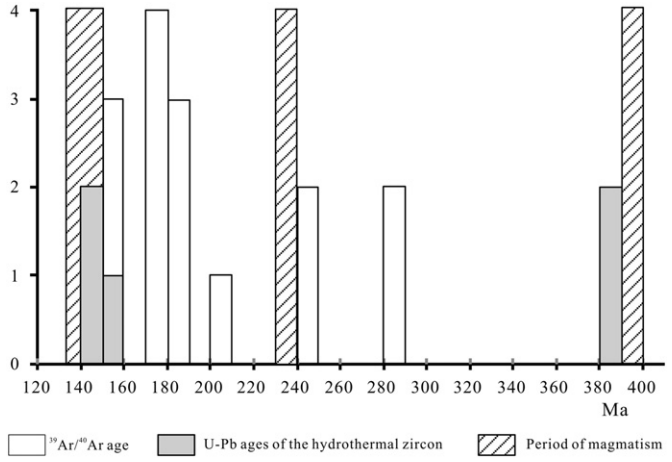

Fig. 8. Comparison of the $^{39}Ar/^{40}Ar$ ages of the K-feldspar, sericite, quartz vein and U–Pb ages of the hydrothermal zircon from the ores, and the regional magmatism. Ages of the magmatic rocks including the Shuiquangou syenite, Honghualiang, the Guzuizi, Shangshuiquan, and Beizhazhi granites, and the Zhuanzhilian diorite (Bao et al., 2014; Jiang et al., 2007; Li and Bao, 2012; Miao et al., 2002). U–Pb ages of the hydrothermal zircons for the Dongping and Hougou gold deposits are from Bao et al. (2014) and Li et al. (2012b). $^{39}Ar/^{40}Ar$ ages for the Dongping, Hougou, Zhongshangou, and Huangtuliang gold deposits are from Lu et al. (1993), Song and Zhao (1996),Jiang and Nie (2000), and Hart et al. (2002).

Therefore, we propose that the Dongping gold deposit may have formed by two stages of hydrothermal fluids at ~385 and ~140 Ma. The first stage of gold mineralization was of late-magmatic hydrothermal origin and was related to the Shuiquangou syenite intrusion, whereas the second stage of gold mineralization was a hydrothermal overprint associated with the Late Jurassic–Early Cretaceous granitic magmatism.

The northern part of the North China Craton was a passive continental margin in Ordovician to Silurian and experienced subduction and subsequent amalgamation of the Ondor Sum accretionary complex (Zhang et al., 2010). The emplacement of the Shuiquangou syenite intrusion along with other alkaline intrusions and mafic–ultramafic complex occurred at the termination of the Early Paleozoic orogenic cycle around the margin of the northern North China Craton (Zhang et al., 2010). The northern part of the North China Craton evolved into a post-collisional extensional regime in the early Devonian (e.g., Zhang et al., 2010 and references therein). At this time, the Dongping gold deposit is formed by hydrothermal processes (~385 Ma) subsequent to the emplacement of the Shuiquangou syenite intrusion (400–386 Ma). The ore-forming fluids exsolved from the syenites and were mixed with meteoric waters. The syenite-derived Au may have migrated as hydrosulfide and/or polytellurides in the high temperature and low salinity ore-forming fluids (Brugger et al., 2012; Cook et al., 2009b; Gammons and Williams-Jone, 1997), and finally deposited due to fluid mixing, cooling, phase separation and the reaction with the wall rocks as indicated by the inclusion results and the extensive silicification and K-feldsparthization. During the Yanshanian orogenic processes in the

Table 5
Results of isotopic dating for the gold deposits related to the Shuiquangou syenite complex.

Sampling location	Mineral or rock analyzed	Method	Age (Ma)	Source
Dongping gold deposit (No.1 to N.70 vein group)	Zircon, disseminated ore	LA-ICP-MS zircon U–Pb	389 ± 1	Bao et al. (2014)
	Zircon, auriferous quartz vein	SIMS zircon U–Pb	385 ± 5.7	Bao et al. (2014)
	Zircon, auriferous quartz vein	Conventional zircon U–Pb	350.9 ± 0.9	Li et al. (1998)
	K-feldspar, disseminated ore	$^{39}Ar/^{40}Ar$	289.1 ± 0.3	Jiang and Nie (2000)
	Sericite, disseminated ore	$^{39}Ar/^{40}Ar$	186.8 ± 0.3	Jiang and Nie (2000)
	K-feldspar, auriferous quartz vein	$^{39}Ar/^{40}Ar$	177.4 ± 5	Song and Zhao (1996)
	K-feldspar, auriferous quartz vein	$^{39}Ar/^{40}A$ r	156.7 ± 0.9	Lu et al. (1993)
	Muscovite, disseminated ore	$^{39}Ar/^{40}Ar$	153 ± 3	Hart et al. (2002)
			153 ± 2	
	Zircon, low grade quartz vein	SIMS zircon U–P	147.8 ± 2.3	Bao et al. (2014)
	Hydrothermal zircon, quartz vein	LA-ICPMS zircon U–Pb	140.3 ± 1.4	Li et al. (2010)
	Fluid-inclusion, auriferous quartz vein	Rb–Sr isochron	103 ± 8	Mo et al. (1997)
Zhongshangou gold deposit	K-feldspar, auriferous altered rocks adjacent to quartz vein	$^{39}Ar/^{40}Ar$	241 ± 1	Hart et al. (2002)
			246 ± 1	
Hougou gold deposit	K-feldspar, auriferous altered rock adjacent to quartz vein	$^{39}Ar/^{40}Ar$	288.1 ± 0.4	Jiang and Nie (2000)
	K-feldspar, auriferous quartz vein	Laser probe $^{39}Ar/^{40}Ar$	202.6 ± 1.0	Xu et al. (2002)
			179.7 ± 1.6	
	Sericite, auriferous altered rock adjacent to quartz vein	$^{39}Ar/^{40}Ar$	187.6 ± 0.4	Jiang and Nie (2000)
	Quartz, auriferous quartz vein	$^{39}Ar/^{40}Ar$	177.6 ± 1.9	Hu and Luo (1994)
	K-feldspar, auriferous quartz vein	$^{39}Ar/^{40}Ar$	172.9 ± 5	Wang (1992)
	Hydrothermal zircon, mylonite	LA-ICPMS U–Pb	154.4 ± 1.3	Li et al. (2012b)
Huangtuliang gold deposit	Sericite, auriferous altered rock adjacent to quartz vein	$^{39}Ar/^{40}Ar$	187.4 ± 0.3	Jiang and Nie (2000)

Late Jurassic–Early Cretaceous, the fluids derived from the extensive granitic magmatism mixed with meteoric waters, and this resulted in the remobilization of the original gold mineralization and resulted second enrichment.

The model that we propose can explain the most important major field relationships and the geochemical variations. The genetic link between the Shuiquangou syenite intrusion and the gold mineralization is consistent with the observation that 13 gold deposits occur within or adjacent to the Shuiquangou syenite intrusion (Li et al., 2000b; Song and Zhao, 1996; Wang et al., 1990; Yin, 1994), whereas there is no gold mineralization related to the abundant Triassic and Jurassic to Cretaceous granite intrusions in the study area (Fig. 8). O, H, Sr and He isotopic compositions of the ore-forming fluids suggest that the fluids were mainly derived from the Shuiquangou syenite intrusion (Fig. 5). In addition, the overlap of $\delta^{34}S$ Pb isotope compositions of the ores and the syenites also manifests a genetic link (Figs. 6,7).

5. Summary

The Dongping deposit and other gold deposits in the Northwestern Hebei Province, China are spatially and temporally associated with the Devonian Shuiquangou syenite intrusion.

(1) The Shuiquangou syenites experienced a prolonged history of crystallization; 400 ± 3.5 Ma in the western part (LA-ICPMS zircon U–Pb) to 386 ± 6 Ma in the eastern part of the intrusion (SHRIMP zircon U–Pb).
(2) There are three major ore types in the deposit, i.e., auriferous quartz vein in the upper part, quartz stockwork and disseminated ores in the middle part, and disseminated ores in the lower part. The ores are characterized by low sulfide, tellurium rich. Gold mainly occurs as native gold, calaverite, electrum, and petzite.
(3) Isotope geochemical and fluid inclusion results show that Au was mainly derived from the syenite intrusion, and accordingly, the ore-forming fluids were primarily magmatic waters with the participation of meteoric waters.
(4) LA-ICPMS and SIMS U–Pb dating of the hydrothermal zircons from the ores demonstrated that the Dongping gold deposit was mainly formed during the late-magmatic hydrothermal stage immediately subsequent to the emplacement of the Shuiquangou syenite intrusion, however, the Late Jurassic–Early Cretaceous hydrothermal overprints also contributed to the gold mineralization in the Dongping deposit and the other gold deposits associated with the syenite intrusion.

Acknowledgments

This study is supported by the National Natural Science Foundation of China (No. 41372083). We are grateful to Cristina Yan Wang and Weidong Sun for their helpful suggestions. The two anonymous reviewers are thanked for their constructive comments. We thank Dr. Peter Lightfoot for his efficient editorial handling of the manuscript. Cenozoic Geoscience Editing is acknowledged for its professional editing and language polishing service.

References

Bao, Z.W., Zhao, Z.H., 2003. Rare-earth element mobility during ore-forming hydrothermal alteration: a case study of Dongping gold deposit, Hebei province, China. Chin. J. Geochem. 22, 45–57.
Bao, Z.W., Zhao, Z.H., 2006. Isotopic geochemical constraints on metallogeny of the Dongping-type gold deposits associated with syenites. Acta Petrol. Sin. 22, 2534–2542 (in Chinese with English abstract).
Bao, Z.W., Zhao, Z.H., Zhou, L.D., Zhou, G.F., 1996. An investigation into the petrogenesis of the Shuiquangou syenite complex, northwest of Hebei province. Acta Petrol. Sin. 12, 562–572 (in Chinese with English abstract).
Bao, Z.W., Zhao, Z.H., Zhang, P.H., Wang, Y.X., 2000. Lead isotopic compositions of the Dongping-type gold deposit and their exploration application. Geochimica 29, 223–230 (in Chinese with English abstract).
Bao, Z.W., Zhao, Z.H., Zhang, P.H., Wang, Y.X., 2003. REE, Sr, Nd, and Pb isotopic evidence for the petrogenesis of the Shuiquangou syenite complex in NW Hebei province, China. Geol. Rev. 49, 621–627 (in Chinese with English abstract).
Bao, Z.W., Sun, W.D., Li, C.J., Zhao, Z.H., 2014. U–Pb dating of hydrothermal zircon from the Dongping gold deposit in North China: constraints on the mineralization processes. Ore Geol. Rev. 61, 107–119.
Brugger, J., Etschmann, B.E., Grundler, P.V., Liu, W.H., Testemale, D., Pring, A., 2012. XAS evidence for the stability of polytellurides in hydrothermal fluids up to 599 °C, 800 bar. Am. Mineral. 97, 1519–1522.
Chen, B., Liu, S.W., Geng, Y.S., Liu, C.Q., 2006. Zircon U–Pb ages, Hf isotopes and significance of the Late Archean–Paleoproterozoic granitoids from the Wutai-Lvliang terrain, North China. Acta Petrol. Sin. 22, 296–304 (in Chinese with English abstract).
Ciobanu, C.L., Cook, N.J., Utsunomiya, S., Kogagwa, M., Green, L., Gilbert, S., Wade, B., 2012. Gold-telluride nanoparticles revealed in arsenic-free pyrite. Am. Mineral. 97, 1515–1518.
Clayton, R.N., 1972. Oxygen isotope exchange between quartz and water. J. Geophys. Res. 77, 3057–3607.
Cook, N.J., Ciobanu, C.L., Mao, J.W., 2009a. Textural control on gold distribution in As-free pyrite from the Dongping, Huangtuliang and Hougou gold deposits, North China Craton (Hebei Province, China). Chem. Geol. 264, 101–121.
Cook, N.J., Ciobanu, C.L., Spy, P.G., Voudouris, P., 2009b. Understanding gold-(silver)-telluride-(selenide) mineral deposits. Episodes 32, 249–263.
Davies, J.H., von Blanckenburg, F., 1995. Slab breakoff: a model of lithosphere detachment and its test in the magmatism and deformation of collisional orogens. Earth Planet. Sci. Lett. 129, 85–102.
Davis, D.W., Krogh, T.E., 2000. Preferential dissolution of ^{238}U and radiogenic Pb from α-recoil-damaged lattice sites in zircon: implications for thermal histories and Pb isotopic fraction in the surface environment. Chem. Geol. 172, 41–85.
Fan, H.R., Xie, Y.H., Zhai, M.G., 2001. Ore-forming fluids in the Dongping gold deposit, northwestern Hebei Province. Sci. China D 44, 748–757.
Fan, H.R., Zhai, M.G., Xie, Y.H., Yang, J.H., 2003. Ore-forming fluids associated with granite-hosted gold mineralization at the Sanshandao deposit, Jiaodong gold province, China. Mineral. Deposita 38, 739–750.
Gammons, C.H., Williams-Jone, A.E., 1997. Chemical mobility of gold in the porphyry-epithermal environment. Econ. Geol. 92, 45–59.
Goldfarb, R.J., Santosh, M., 2014. The dilemma of the Jiaodong gold deposits: are they unique? Geosci. Front. 5, 139–153.
Goldfarb, R.J., Groves, D.I., Gardoll, S., 2001. Orogenic gold and geologic time: a global synthesis. Ore Geol. Rev. 18, 1–75.
Hart, C.J.R., Goldfarb, R.J., Qiu, Y.M., Snee, L., Miller, L.D., Miller, M.L., 2002. Gold deposits of the northern margin of the North China Craton: multiple late Paleozoic–Mesozoic mineralizing events. Mineral. Deposita 37, 326–351.
Helt, K.M., Williams-Jones, A.E., Clark, J.R., Wing, B.A., Wares, R.P., 2014. Constraints on the genesis of the Archean oxidized, intrusion-related Canadian Malartic gold deposit, Quebec, Canada. Econ. Geol. 109, 713–735.
Hu, D.X., Luo, G.L., 1994. $^{40}Ar/^{39}Ar$ ages of gold-bearing quartz veins and their geological significance in typical gold deposits of Zhangjiakou-Xuanhua gold field, Hebei province. Sci. Geol. Sin. 29, 151–158 (in Chinese with English abstract).
Hu, L., Song, H.L., 2002. Age of activities of the southern "Inner Mongolian axis" marginal fault belt and an analysis of its structure. Chin. Geol. 29, 369–373 (in Chinese with English abstract).
Hu, F.F., Fan, H.R., Zhai, M.G., Jin, C.W., 2006a. Fluid evolution in the Rushan lode gold deposit of Jiaodong Peninsula, eastern China. J. Geochem. Explor. 89, 161–164.
Hu, H.B., Mao, J.W., Niu, S.Y., Li, Y.F., Li, M.W., 2006b. Geology and geochemistry of telluride bearing Au deposits in the Pingyi area, Western Shandong, China. Mineral. Petrol. 87, 209–240 (in Chinese with English abstract).
Jensen, E.P., Barton, M.D., 2000. Gold deposits related to alkaline magmatism. Rev. Econ. Geol. 13, 279–314.
Jiang, N., 2005. Petrology and geochemistry of the Shuiquangou syenitic complex, northern margin of the North China Craton. J. Geol. Soc. Lond. 162, 203–215.
Jiang, N., 2006. Hydrothermal alteration of chevkinite-(Ce) in the Shuiquangou syenitic intrusion, northern China. Chem. Geol. 227, 100–112.
Jiang, S.H., Nie, F.J., 1998. A comparison study on geological and geochemical features and ore genesis of the Xiaoyingpan and Dongping gold deposits, Hebei. Gold Geol. 4 (4), 12–24 (in Chinese with English abstract).
Jiang, S.H., Nie, F.J., 2000. $^{40}Ar/^{39}Ar$ geochronology study on the alkaline intrusive complex and related gold deposits, northwestern Hebei, China. Geol. Rev. 46, 621–627 (in Chinese with English abstract).
Jiang, S.H., Nie, F.J., 2003. Nd-isotope constraints on origin of the Shuiquangou intrusive complex, North-Western Hebei, China. Geol. Rev. 49, 355–360 (in Chinese with English abstract).
Jiang, X.M., Fan, B.H., Li, S.Z., 2000. Gold ore controlling structure in Dongping gold ore field, Chongli County, Hebei Province, China. Contrib. Geol. Miner. Resour. Res. 15, 351–356 (in Chinese with English abstract).
Jiang, N., Sun, S.H., Chu, X.L., Mizutab, T., Ishiyama, D., 2003. Mobilization and enrichment of high-field strength elements during late and post-magmatic processes in the Shuiquangou syenitic complex, Northern China. Chem. Geol. 200, 117–128.
Jiang, N., Liu, Y.S., Zhou, W.G., Yang, J.H., Zhang, S.Q., 2007. Derivation of Mesozoic adakitic magmas from ancient lower crust in the North China craton. Geochim. Cosmochim. Acta 71, 2591–2608.
Jiang, N., Guo, J.H., Zhai, M.G., Zhang, S.Q., 2010. ~2.7 Ga crust growth in the North China Craton. Precambrian Res. 179, 37–49.

Kelly, K.D., Ludington, S., 2002. Cripple Creek and other alkaline-related gold deposits in the southern Rocky Mountains, USA: influence of regional tectonics. Mineral. Deposita 37, 38–60.
Li, C.M., 1999. Relationship between the gold source of Dongping gold deposit and Archean TTG-greenstone belt. Prog. Precambrian Res. 22, 40–46 (in Chinese with English abstract).
Li, C.J., Bao, Z.W., 2012. Geochemical characteristics and geodynamic implications of the Early Cretaceous magmatisms in Zhangjiakou region, northwest Hebei Province, China. Geochimica 41, 343–358 (in Chinese with English abstract).
Li, H.M., Li, H.K., Lu, S.N., Yang, C.L., 1998. Determination of age of gold mineralization of Dongping gold deposits by U–Pb dating hydrothermal zircons from ore veins. Acta Geosci. Sin. 18 (sup), 176–178 (in Chinese).
Li, H.K., Lu, S.N., Li, H.M., Yang, C.L., 1999. Advancement on the geochronology of the Precambrian basement and mineralization in the Zhangxuan gold concentrated region. Acta Geosci. Sin. 20, 169–176 (in Chinese with English abstract).
Li, H.Y., Zhang, Z.Y., Li, P., Xing, G.H., 2000a. Structural analysis and genesis of gold deposit in the Dongping. Geol. Prospect. 36 (5), 36–38 (in Chinese with English abstract).
Li, H.Y., Yang, Z.S., Ding, Z.J., Luo, T.Y., Gao, Z.M., 2000b. Characteristics of geochemistry in the Jinjiazhuang ultramafic rock-type gold deposit in Chicheng county, Hebei province. Geol. Prospect. 36 (4), 24–27 (in Chinese with English abstract).
Li, J.L., Makovicky, E., Rose-Hansen, J., Peterson, S.B., Qi, F., Cui, Y.H., Xu, Q.S., 2001. Mustard gold and its varieties from Dongping mine, Hebei Province, China. Geoscience 15, 189–196 (in Chinese with English abstract).
Li, C.M., Deng, J.F., Chen, L.H., Su, S.G., Li, H.M., Hu, S.L., 2010. Two periods of zircon from Dongping gold deposit in Zhangjiakou-Xuanhua area, northern margin of North China: constraints on metallogenic chronology. Mineral. Deposita 29, 265–275 (in Chinese with English abstract).
Li, C.J., Bao, Z.W., Zhao, Z.Z., Qiao, Y.L., 2012a. Zircon U–Pb age and Hf isotopic compositions of the granitic gneisses from the Sanggan complex in the Zhangjiakou area: Constraints on the early evolution of North China Craton. Acta Petrol. Sin. 28, 1057–1072 (in Chinese with English abstract).
Li, C.M., Deng, J.F., Su, S.G., Liu, X.M., 2012b. LA-ICP-MS zircon U–Pb age of the brittle-ductile shear zones in Hougou gold orefield, Northwestern Hebei Province. Geotecton. Metallog. 36, 157–167 (in Chinese with English abstract).
Liang, H.Y., Mo, C.H., Wang, X.Z., 1998. Single zircon Pb-evaporation age of Shuiquangou gold-bearing alkali-intrusion in Zhangjiakou area, Hebei Province. Chin. J. Geochem. 17, 152–158.
Liu, Z.F., Wang, J.M., Lv, J.B., Zheng, G.S., 2006. Geological features and age of the Wenquan rapakivi granite, Chicheng County, Hebei. Geol. China 33, 1052–1058 (in Chinese with English abstract).
Liu, S.W., Lv, Y.J., Feng, Y.G., Zhang, C., Tian, W., Yan, Q.R., Liu, X.M., 2007. Geology and zircon U–Pb isotopic chronology of Dantazi complex, northern Hebei Province. Geol. J. China Univ. 13, 484–497 (in Chinese with English abstract).
Lu, D.L., 1991. Study on the genesis and ore controlling structures of the Dongping gold deposit in Chongli county, Hebei province. Unpublished geological report (in Chinese).
Lu, D.L., Wang, J.J., Luo, X.Q., Zhang, S.H., Zheng, B.Y., 1993. The metallogenic epoch of the Dongping gold deposit. Mineral Deposits 12, 182–188 (in Chinese with English abstract).
Lu, H.Z., Guy, A., Li, Y.S., 1997. Deformation style and shear zone control gold mineralization in Dongping area, Hebei Province, China. J. Guilin Inst. Technol. 17, 316–323 (in Chinese with English abstract).
Ma, Z.J., Zhao, J.M., 1999. Contrast research on Tianshan orogenic belt and Yinshan–Yanshan orogenic belt. Earth Sci. Front. 6, 95–102 (in Chinese with English abstract).
Macfarlane, A.W., Petersen, U., 1990. Pb isotopes of the Hualgayoc area, Northern Peru: implications for metal provenance and genesis of a Cordilleran polymetallic mining district. Econ. Geol. 85, 1303–1327.
Mao, J.W., Li, Y.Q., 2001. Fluid inclusions of the Dongping gold telluride deposit in Hebei Province, China: Involvement of mantle fluid in metallogenesis. Mineral Deposits 20, 23–36 (in Chinese with English abstract).
Mao, J.W., Li, Y.Q., Goldfarb, R., He, Y., Zaw, K., 2003. Fluid inclusions and noble gas studies of the Dongping gold deposit, Hebei Province, China: a mantle connection for mineralization? Econ. Geol. 98, 517–534.
Masuda, A., Ikeuchi, Y., 1979. Lanthanide tetrad effect observed in marine environment. Geochem. J. 13, 19–22.
Miao, L.C., Qiu, Y.M., McNaughton, N., Luo, Z.K., Groves, D., Zhai, Y.S., Fan, W.M., Zhai, M.G., Guan, K., 2002. SHRIMP U–Pb zircon geochronology of granitoids from Dongping area, Hebei Province, China: constraints on tectonic evolution and geodynamic setting for gold metallogeny. Ore Geol. Rev. 19, 187–204.
Miller, L.D., Goldfarb, R.J., Nie, F.J., Hart, C.J.R., Miller, M.L., Yang, Y., Liu, Y., 1998. North China gold. A product of multiple orogens. SEG Newsl. 33 (1), 6–12.
Mo, C.H., Wang, X.Z., Cheng, J.P., Liang, H.Y., 1997. Rb–Sr isochron determination for fluid inclusions within quartz vein from Dongping gold deposit, NW Hebei Province and its implications for metallogeny. Geochimica 26 (3), 20–27 (in Chinese with English abstract).
Monecke, T., Kempe, U., Monecke, J., Sala, M., Wolf, D., 2002. Tetrad effect in rare earth element distribution patterns: a method of quantification with application to rock and mineral samples from granite-related rare metal deposits. Geochim. Cosmochim. Acta 66, 1185–1196.
Nie, F.J., 1998. Geology and origin of the Dongping alkalic-type gold deposit, Northern Hebei Province, People's Republic of China. Resour. Geol. 48, 139–158.
Nie, F.J., Jiang, S.H., Liu, Y., 2004. Intrusion-related gold deposits of North China craton, People's Republic of China. Resour. Geol. 54, 299–324.
Nimis, P., Omenetto, P., Giunti, I., Artioli, G., Angelini, I., 2012. Lead isotope systematics in hydrothermal sulphide deposits from the central-eastern Southalpine (northern Italy). Eur. J. Mineral. 24, 23–37.
Ohmoto, H., 1972. Systematics of sulfur and carbon in hydrothermal ore deposits. Econ. Geol. 67, 551–579.
Ohmoto, H., Rye, R.O., 1979. Isotopes of sulfur and carbon. In: Barnes, H.L. (Ed.), Geochemistry of Hydrothermal Ore Deposits, 2nd ed. Wiley, New York, pp. 509–567.
Robert, F., 2001. Syenite-associated disseminated gold deposits in the Abitibi greenstone belt, Canada. Mineral. Deposita 36, 503–516.
Rudnick, R.L., Gao, S., 2003. Composition of the Continental Crust. In: Rudnick, R.L. (Ed.), The Crust. Elsevier, Oxford, pp. 1–64.
Sillitoe, R.H., 2002. Some metallogenic features of gold and copper deposits related to alkaline rocks and consequences for exploration. Mineral. Deposita 37, 4–13.
Song, G.R., Zhao, Z.H., 1996. Geology of Dongping Alkaline Complex-hosted Gold Deposit in Hebei Province. Seismological Press, Beijing, pp. 1–170 (in Chinese with English abstract).
Sun, S.S., McDonough, W.F., 1989. Chemical and isotopic systematics of oceanic basalts: implications for mantle composition and processes. In: Saunders, A.D., Norry, M.J. (Eds.), Magmatism in the Ocean Basins. Geol. Soc. London, London, pp. 313–345.
Sun, W.D., Ding, X., Hu, Y.H., Li, X.H., 2007. The golden transformation of the Cretaceous plate subduction in the west Pacific. Earth Planet. Sci. Lett. 262, 533–542.
Sun, W.D., Liang, H.Y., Ling, M.X., Zhan, M.Z., Ding, X., Zhang, H., Yang, X.Y., Li, Y.L., Ireland, T.R., Wei, Q.R., Fan, W.M., 2013. The link between reduced porphyry copper deposits and oxidized magmas. Geochim. Cosmochim. Acta 103, 263–275.
Taylor Jr., H.P., 1997. Oxygen and hydrogen isotope relationship in hydrothermal mineral deposits. In: Barnes, H.L. (Ed.), Geochemistry of Hydrothermal Ore Deposits, 3rd edition John Wiley & Sons Co., Danvers, pp. 229–302.
Tian, S.Z., Li, X., 1995. A preliminary study of some new minerals in Dongping gold deposit, Hebei Province. Gold Geol. 1, 61–67 (in Chinese with English abstract).
Tian, W., Chen, B., Liu, C.Q., Zhang, H.F., 2007. Zircon U–Pb age and Hf isotopic composition of the Xiaozhangjiakou ultramafic pluton in northern Hebei. Acta Petrol. Sin. 23, 583–590 (in Chinese with English abstract).
Villa, I.M., Williams, M.L., 2013. Geochronology of metasomatic events. In: Harlov, D.E., Austrheim, H. (Eds.), Metasomatism and the Chemical Transformation of Rock, Lecture Notes in Earth System Sciences. Springer-Verlag, Berlin Heidelberg, pp. 171–202.
Wang, R.R., 1992. The characteristics and genesis of the felsic alkali complex, Jinjiazhuang, Hebei. J. Guilin Inst. Technol. 12, 12–20 (in Chinese with English abstract).
Wang, Y., Meng, H.J., 2000. Study of the gold minerals in Dongping gold mine, Hebei, China. Contrib. Geol. Miner. Resour. Res. 15, 51–63 (in Chinese with English abstract).
Wang, Y., Jiang, X.M., Wang, Z.K., 1990. Characteristics of lead and sulfur isotope of the gold deposits in Zhangjiakou Xuanhua area, Hebei Province. Contrib. Geol. Miner. Resour. Res. 5 (2), 66–75 (in Chinese with English abstract).
Wang, Z.K., Jiang, X.M., Wang, Y., Shang, M.Y., 1992. A comparative analysis on geological–geochemical features of the Xiaoyingpan and Dongping gold deposits, Hebei. Geol. Prospect. 28 (7), 14–20 (in Chinese with English abstract).
Wang, Y., Jiang, X.M., Shang, M.Y., Wang, Z.K., 1994. The geological characteristics and origin of gold deposits related to subalkaline rocks in northern Hebei Province. Geol. Rev. 40, 368–376 (in Chinese with English abstract).
Wang, F., Chen, F.K., Siebel, W., Li, S.Q., Peng, P., Zhai, M.G., 2011. Zircon U–Pb geochronology and Hf isotopic composition of the Hongqiyingzi Complex, northern Hebei Province: new evidence for Paleoproterozoic and late Paleozoic evolution of the northern margin of the North China Craton. Gondwana Res. 20, 122–136.
Wilkinson, J.J., 2001. Fluid inclusions in hydrothermal ore deposits. Lithos 55, 229–272.
Wu, S.S., 2009. Research on ore-formation and ore-controlling structure of Zhongshangou gold deposit in Chongli county, Hebei province [MS] Shijiazhuang University of Economics. 1-71 (in Chinese with English abstract).
Wyman, D., Kerrich, R., 1988. Alkaline magmatism, major structures, and gold deposits: implication for greenstone belt gold metallogeny. Econ. Geol. 83, 454–461.
Xiang, S.Y., Ye, J.L., Liu, J., 1992. The genesis of Hougou-Shuiquangou alkali-syenite rock mass and the relation between it and the mineralization of gold deposits. Geoscience 6, 55–62 (in Chinese with English abstract).
Xing, W.W., Li, F., Liu, X.H., Yang, Y.S., Cheng, Y., 2011. Characteristics and mineralizaiton of Shuijingtun gold deposit in Chongli county, Hebei province. Gansu Geol. 20 (2), 51–59 (in Chinese with English abstract).
Xu, X.W., Cai, X.P., Liu, Y.L., Zhang, B.L., 2002. Laser probe ^{40}Ar-^{39}Ar ages of metasomatic K-feldspar from the Hougou gold deposit, northwestern Hebei Province, China. Sci. China D 45, 559–564.
Yang, J.H., Wu, F.Y., Wilde, S.A., 2003. A review of the geodynamic setting of large-scale Late Mesozoic gold mineralization in the North China Craton: an association with lithospheric thinning. Ore Geol. Rev. 23, 125–152.
Yin, J.Z., 1994. S isotopic features of the major gold deposits in the Northwestern Hebei Province. Gold Sci. Technol. 2 (3), 33–39 (in Chinese).
Yin, J.Z., Zhai, Y.S., 1994. On the metallogenic series of gold deposits in Zhangjiakou-Xuanhua region, Hebei. J. Guilin Coll. Geol. 14, 359–369 (in Chinese with English abstract).
Zartman, R.E., Haines, S.M., 1988. The plumbotectonic model for Pb isotopic systematics among major terrestrial reservoirs — a case for bi-directional transport. Geochim. Cosmochim. Acta 52, 327-1339.
Zhai, M.G., Santosh, M., 2011. The early Precambrian odyssey of North China Craton: a synoptic overview. Gondwana Res. 20, 6–25.
Zhai, M.G., Santosh, M., 2013. Metallogeny of the North China Craton: link with secular changes in the evolving Earth. Gondwana Res. 24, 275–297.
Zhai, M.G., Yang, J.H., Fan, H.R., Miao, L.C., Li, Y.G., 2002. A large-scale cluster of gold deposits and metallogenesis in the eastern North China Craton. Int. Geol. Rev. 44, 458–476.
Zhang, Z.C., Mao, J.W., 1995. Geology and geochemistry of the Dongping gold telluride deposit, Hebei Province, North China. Int. Geol. Rev. 37, 1094–1108.

Zhang, P.H., Zhao, Z.H., Bao, Z.W., Wang, Y.X., Niu, H.C., Zhao, W.X., Gu, X.P., Lai, M.Y., 2000. $H_2Pb_2Fe_4[(Te, S)O_4]_9 \cdot 9H_2O$: a undesignated tellurite mineral from the Dongping gold deposit. Bull. Mineral. Petrol. Geochem. 19, 356–359 (in Chinese).

Zhang, P.H., Zhao, Z.H., Bao, Z.W., Wang, Y.X., Li, S.Z., Zhang, Y.H., 2001. The distribution pattern of gold and tellurium and their correlation of ores from the Dongping gold mine. Geol. Prospect. 37 (3), 24–28 (in Chinese with English abstract).

Zhang, P.H., Zhao, Z.H., Zhu, J.C., Zhang, W.L., Bao, Z.W., Zhang, Y.H., 2002a. Tellurides of gold and silver and their capacity of carrying gold in ores from the Dongping type gold deposits, Hebei Province, China. Acta Mineral. Sin. 22, 321–328 (in Chinese with English abstract).

Zhang, P.H., Zhu, J.C., Zhao, Z.H., Lu, L., Liu, D., 2002b. Oxidation and dissolution of calaverites in Dongping gold deposit under supergene conditions. Mineral Deposits 21 (Suppl.), 783–786 (in Chinese).

Zhang, P.H., Zhu, J.C., Zhao, Z.H., Gu, X.P., Lin, J.F., 2004. Zincospiroffite, a new tellurite mineral species from the Zhongshangou gold deposit, Hebei Province, People's Republic of China. Can. Mineral. 42, 763–768.

Zhang, J.H., Jiang, S.H., Nie, F.J., 2005. Geological features of the Hougou and Huangtuliang gold deposits, northwestern Hebei Province. In: Jiang, S.H., Zhang, J.H., Nie, F.J. (Eds.), Field Trip Guide No. 7, Intrusion-Related Gold Deposits of the Northern Margin of the North China Craton, Hebei Province, China, 8th Biennial SGA Meeting, 18–21 August 2005, Beijing, China, p. 12.

Zhang, S.H., Zhao, Y., Liu, J., Hu, J.M., Chen, Z.L., Pei, J.L., Chen, Z.Y., Zhou, J.X., 2007. Emplacement depths of the Late Paleozoic–Mesozoic granitoid intrusions from the northern North China block and their tectonic implications. Acta Petrol. Sin. 23, 625–638 (in Chinese with English abstract).

Zhang, X.H., Zhang, H.F., Jiang, N., Zhai, M.G., Zhang, Y.B., 2010. Early Devonian alkaline intrusive complex from the northern North China craton: a petrological monitor of post-collisional tectonics. J. Geol. Soc. Lond. 167, 717–730.

Zhang, G.R., Xu, J.H., Wei, H., Song, G.C., Zhang, Y.B., Zhao, J.K., Chen, D.L., 2012. Structure, alteration, and fluid inclusion study on deep and surrounding area of the Dongping gold deposit, northern Hebei, China. Acta Petrol. Sin. 28, 637–651 (in Chinese with English abstract).

Zhao, Z.H., Bao, Z.W., Qiao, Y.L., 2010. A peculiar composite M- and W-type REE tetrad effect: Evidence from the Shuiquangou alkaline syenite complex, Hebei Province, China. Chin. Sci. Bull. 55, 2684–2696.